A 2D-3D Registration Framework for Freehand TRUS-Guided Prostate Biopsy

Siavash Khallaghi[1], C. Antonio Sánchez[1], Saman Nouranian[1],
Samira Sojoudi[1], Silvia Chang[2], Hamidreza Abdi[3], Lindsay Machan[2], Alison
Harris[2], Peter Black[3], Martin Gleave[3], Larry Goldenberg[3], and S. Sidney Fels[1],
and Purang Abolmaesumi[1]

Department of Electrical and Computer Engineering, University of British Columbia,
Vancouver, Canada
Vancouver General Hospital, Vancouver, Canada
Department of Urological Sciences, Vancouver, Canada
{siavashk,antonios}@ece.ubc.ca

Abstract. We present a 2D to 3D registration framework that compensates for prostate motion and deformations during freehand prostate biopsies. It has two major components: 1) a trajectory-based rigid registration to account for gross motions of the prostate; and 2) a non-rigid registration constrained by a finite element model (FEM) to adjust for residual motion and deformations. For the rigid alignment, we constrain the ultrasound probe tip in the live 2D imaging plane to the tracked trajectory from the pre-procedure 3D ultrasound volume. This ensures the rectal wall approximately coincides between the images. We then apply a FEM-based technique to deform the volume based on image intensities. We validate the proposed framework on 10 prostate biopsy patients, demonstrating a mean target registration error (TRE) of 4.63 mm and 3.15 mm for rigid and FEM-based components, respectively.

1   Introduction

Prostate biopsy is the gold standard for prostate cancer (PCa) diagnosis. This is typically performed freehand using 2D transrectal ultrasound (TRUS) guidance. Unfortunately, the current systematic biopsy approach is prone to false negatives [9], and patients are frequently asked to repeat the procedure. To improve the cancer yield, 3D biopsy systems have been developed [1,4,12]. In these systems, biopsy locations are planned and recorded with respect to a 3D-TRUS reference volume acquired just prior to the procedure. However, the prostate moves and deforms during the biopsy process, in a way which cannot be compensated for using passive tracking alone [1,4,12]. As a result, slice-to-volume registration is required to maintain alignment of the 2D imaging plane with respect to the pre-procedure 3D-TRUS. The goal of this paper is to provide the registration tools to perform such freehand 3D-guided prostate biopsies.

Robust 2D-3D TRUS registration in a freehand environment is challenging. First, an accurate volume representing the prostate "at rest" must be generated.

For freehand biopsies, this volume is typically acquired using a tracked axial sweep from base to apex [7,12]. Unfortunately, due to patient discomfort and inconsistent probe pressure, resulting volumes suffer from deformation artifacts. To reduce these, systems have been developed that use mechanical stabilization [4] or 3D probes [1], ensuring consistent probe pressure. The second challenge relates to the nature of the 2D-3D registration problem. The limited 2D spatial information, low signal-to-noise ratio of TRUS, and varying probe-induced pressures, all make motion and deformation compensation difficult. When the probe is mechanically stabilized, De Silva *et al.* [4,3] show that rigid 2D-3D registration is sufficient for 3D guidance. They approximate the prostate as rigid, and its motion is learned based on probe positions/orientations [3]. Systems that use 3D probes [1] avoid the 2D-3D registration issue, since the additional out-of-plane information can be used to increase accuracy and robustness [2,7]. However, neither mechanical systems nor 3D probes are widely used in clinics. A solution for freehand 3D-guidance using 2D-TRUS probes, as part of the current standard-of-care, is highly desirable.

In this paper, we provide a solution for freehand TRUS-guided prostate biopsies using a combined rigid and non-rigid 2D-3D registration. The closest works to ours, involving slice-to-volume registration on freehand TRUS data, are by Xu *et al.* [12] and Khallaghi *et al.* [7]. The shortcoming in Xu *et al.* [12] is that their method does not compensate for non-rigid prostate deformations, and target registration error (TRE) is only evaluated on phantom studies. Khallaghi *et al.* [7] compensate for deformations using a B-spline approach. However, their validation is on axial slices of TRUS images acquired in a similar motion as the pre-procedure sweep, leading to a simpler problem. It has not been applied to TRUS slices obtained from arbitrary orientations.

In the absence of strong prior knowledge of prostate motion, even rigid 2D-3D registration often does not converge. To improve robustness, Baumann *et al.* [1] constrain the registration using a manually delineated bounding ellipsoid approximating the prostate shape. This provides a boundary condition for rectal probe kinematics. We follow a similar approach. However, in our case the rigid registration is constrained using the trajectory of the tracked probe's tip during the freehand sweep. This ensures that the rectal wall in both the slice and volume are approximately aligned. We then compensate for residual motion and deformation using a non-rigid 2D-3D registration based on a finite element model (FEM). This incorporates physical prior knowledge, since deformations during a prostate biopsy are mostly probe-induced, and therefore biomechanical in nature. FEM-based methods have been previously applied to 3D-3D registration [5,10,11], but these use the FEM as part of a forward transformation model: from source to the target image. When the target is a 2D slice, this requires scattered data interpolation from the warped volume onto the slice plane, which can be computationally expensive. To alleviate this issue, we propose a backward transformation model that maps the regular 2D grid on the slice directly to the 3D volume. To the best of our knowledge, this is the first report of a FEM-based 2D-3D registration for freehand prostate biopsies.
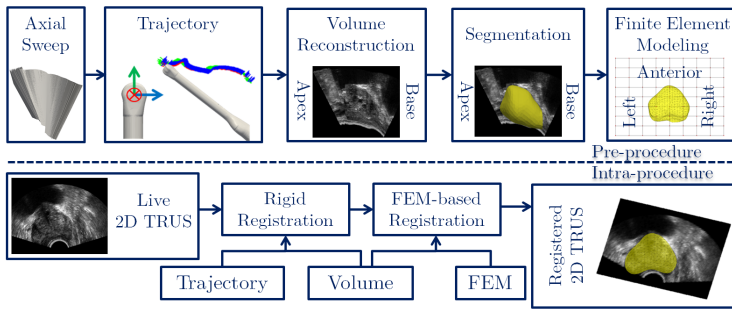
Fig. 1. Clinical workflow. Pre-procedure: The radiologist takes a freehand sweep of the prostate gland from base to apex (frame stack shown in gray). This sweep is used to construct a probe tip trajectory and a 3D volume (sagittal view). This volume is segmented to create a FEM consisting of two regions: the prostate, and the surrounding soft tissue. Intra-procedure: The 2D-TRUS is registered using a rigid transform constrained by the trajectory. Subsequently, a FEM-based non-rigid registration is used to compensate for residual deformations.

2   Methods

2.1   Data Acquisition

The TRUS images in this study were acquired using a magnetically tracked EC9-5/10 probe with a custom data collection software running on a Sonix Touch machine (Ultrasonix Inc., Canada). Prior to the procedure, the probe was calibrated at a depth of 6.0 cm with an N-wire phantom using fCal [8] (calibration accuracy of 0.45 ± 0.2 mm). At the start of the procedure, we asked an interventional radiologist to perform a freehand axial sweep of the prostate gland, from base to apex. We refer to the tracked probe's tip along the sweep as the *trajectory*. This trajectory is shown graphically with red/green/blue axes in Figure 1. Each sweep was obtained at 20 frames/second (≈ 500 frames total), and used to reconstruct a 3D volume of the prostate and surrounding tissue. To account for small fluctuations in probe pressure during the pre-procedure sweep, a moving average with window length of 65 was applied to the transforms. Since the prostate is known to be stiffer than the surrounding tissue [6], we manually segmented the prostate in the 3D-TRUS and created a simplied FEM consisting of two regions: prostate, and the surrounding tissue (see Section 2.2). If desired, segmentation can be automated [13], or skipped and a single homogeneous FEM can be used [10]. Note that commercial 3D-TRUS systems, such as UroNav (Invivo Co., USA) and Artemis (Eigen Inc., USA) already incorporate intra-operative segmentation of the prostate on TRUS images. If elastography becomes part of the prostate biopsy protocol, spatially-varying material properties can also easily be incorporated into the FEM.

Throughout the procedure, tracked TRUS images were obtained continuously at 20 frames/second. At each biopsy location, we asked the radiologist to press

a foot-pedal to tag the TRUS image associated with the core. The 2D-TRUS at each biopsy core was used then for off-line validation of our framework. The two major components are the rigid registration, and the FEM-based deformable registration methods, which are discussed in Section 2.2. We refer to the pre-procedure 3D-TRUS and the intra-procedure 2D-TRUS as source and target images, respectively. A full workflow is presented in Figure 1.

2.2   2D-3D Registration

The 2D-3D registration is framed as the minimization of an objective functional between the planar 2D target image, $F(x) : \mathbb{R}^3 \to \mathbb{R}$, and the 3D source, $M(x) : \mathbb{R}^3 \to \mathbb{R}$, where $x \in \Omega$ refers to grid points on the target slice. We denote the number of points in Ω by N and concatenate them into a single $3N \times 1$ vector, $\boldsymbol{x}$. Since the problem is mono-modal, we used the sum-of-squared differences (SSD) for the intensity metric. For rigid registration, the transform is constrained using the probe trajectory. For FEM-based registration, the objective functional is regularized using the total strain energy of the FEM.

Trajectory-Based Rigid Registration: We formulate the rigid registration as the minimization of the objective functional:

$$Q_{\mathrm{r}}(s, \theta_1, \theta_2, \theta_3) = \frac{1}{2N} \left\| F(\boldsymbol{x}) - M(T_{\mathrm{r}}(s, \theta_1, \theta_2, \theta_3, \boldsymbol{x})) \right\|^2, \qquad (1)$$

where $T_{\mathrm{r}}(s, \theta_1, \theta_2, \theta_3, x)$ is a rigid transform. The translation component is restricted to the probe tip trajectory parameterized by $s \in [0, 1]$. This trajectory approximates the rectal wall in the 3D volume, on which the probe tip in the live 2D imaging plane should also fall. Rotation around the probe tip is controlled by the three Euler angles $(\theta_1, \theta_2, \theta_3)$. To initialize the location parameter s, we project the tracked probe tip to the trajectory. The rotation is initialized using the orientation from magnetic tracking. We then used the "pattern search" optimizer in Matlab (MathWorks, USA) to find the optimal rigid parameters $(s, \theta_1, \theta_2, \theta_3)$.

FEM-Based Registration: Central to the deformable registration is a FEM, constructed from the 3D image volume using a $8 \times 8 \times 8$ grid of hexahedral elements. For simplicity, we use a linear material, which depends on a Young's Modulus, E, and Poisson's ratio, ν. Since the prostate more stiff than the surrounding tissue, we increase the Young's Modulus within this region. Similar to [10], we do not assume any boundary conditions; the FEM is freely able to move based on image-driven forces. We systematically compute the stiffness matrix of the FEM, $K_{3J \times 3J}$, where J is the number of FEM nodes in the hexahedral grid. We formulate the objective functional as a regularized SSD metric:

$$Q_{\mathrm{FEM}}(\boldsymbol{u}) = \frac{1}{2N} \left\| F(\boldsymbol{x}) - M(\boldsymbol{x} - \varPhi\boldsymbol{u}) \right\|^2 + \frac{\alpha}{2} \left\| \boldsymbol{u} - \boldsymbol{u}^{(p)} \right\|^2 + \frac{\beta}{2} \boldsymbol{u}^{\mathsf{T}} K \boldsymbol{u}, \qquad (2)$$

where $\boldsymbol{u}_{3J \times 1} = (u_{11}, \ldots, u_{13}, \ldots, u_{J3})^{\mathsf{T}}$ is the vector of FEM node displacements. A damping term is added for stability, scaled by a coefficient α, that limits deviation from the previous displacement values, $\boldsymbol{u}^{(p)}$. Deformation is controlled

by the strain energy, scaled by regularization weight β. The interpolation matrix, $\Phi_{3N \times 3J}$, is used to represent spatial coordinates $\boldsymbol{x}$ in terms of the FEM node locations. It is constructed by detecting which deformed element contains each point, x, and computing interpolation coefficients based on the element's shape functions (similar to computing barycentric coordinates). Differentiating Equation (2) with respect to the lth coordinate of node k, u_{kl}, yields

$$\frac{\partial Q}{\partial u_{kl}} = \frac{1}{N} \sum_{n=1}^{N} [F_n(\boldsymbol{x}) - M_n(\boldsymbol{y})] \sum_{m=1}^{3} \frac{\partial M_n(\boldsymbol{y})}{\partial y_{nm}} \left(\Phi_{nk} + \sum_{j=1}^{J} \frac{\partial \Phi_{nj}}{\partial u_{kl}} u_{jm} \right)$$

$$+ \alpha \left(u_{kl} - u_{kl}^{(p)} \right) + \beta \sum_{j=1}^{J} \sum_{m=1}^{3} K_{(3k+l)(3j+m)} u_{jm}, \tag{3}$$

where $\boldsymbol{y} = \boldsymbol{x} - \Phi\boldsymbol{u}$ are the mapped coordinates in the moving image volume, n loops over all pixels in the fixed image plane, m loops over the three dimensions, and j loops over all FEM nodes. The derivative of the shape functions with respect to nodal displacements, $\partial \Phi_{nj} / \partial u_{kl}$, can be derived based on the FEM shape functions. By differentiating Equation (2) for all coordinates (k, l) and setting them to zero, we arrive at the sparse linear system:

$$(\Gamma + \alpha I + \beta K)\, \boldsymbol{u} = \Upsilon + \alpha \boldsymbol{u}^{(p)}, \tag{4}$$

where Υ and Γ are defined by collecting the appropriate terms from Equation (3). For the implementation, it is useful to note that if a point $\boldsymbol{x}_n$ falls in an element, then $\Phi_{nk} = \partial \Phi_{nk}/\partial u_{il} = 0$ for all nodes i not belonging to that element. Still, computation of Υ and Γ is the most time-consuming portion of our registration. For each point x, it requires finding the element containing that point, and determining its interpolation functions and their derivatives within the element. We use a bounding volume hierarchy to accelerate the element-detection component. To further improve efficiency, Υ and Γ can be computed in parallel per pixel.

For linear materials, it can be shown that the stiffness matrix scales linearly with the Young's modulus. As a result, the Young's modulus can be factored out and combined with β to create a single free parameter. This means that the proposed registration method has four free parameters: damping coefficient (α), relative soft tissue to prostate elasticity (E_t/E_p), scaled prostate elasticity (βE_p) and Poisson's ratio (ν). Throughout the experiments, we used the following values: $\alpha = 1.0$, $\beta E_p = 0.25 \times 5.0$ kPa [6], $E_t/E_p = 0.2$ [6], $\nu = 0.49$ [10]. The damping parameter, α, prevents large gradients from inducing too strong a force. It should be set large enough to maintain stability, but not too large or it will reduce the convergence rate. The scale parameter, β, controls the relative influence of the image-driven forces and the restoring energy of the FEM. We tuned this parameter to allow realistic deformations. The same parameter values were used for all subjects.
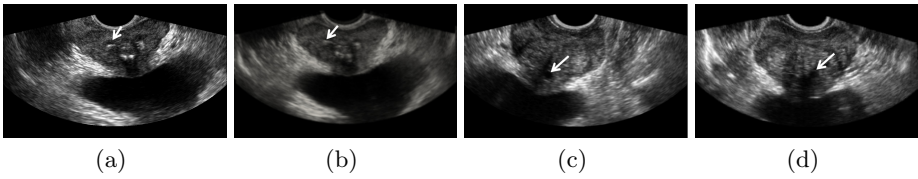
| (a) | (b) | (c) | (d) |

Fig. 2. Example of a calcification (a) and a cyst (c) on the target slice. The corresponding fiducial on the source volume is shown in (b) and (d), respectively.
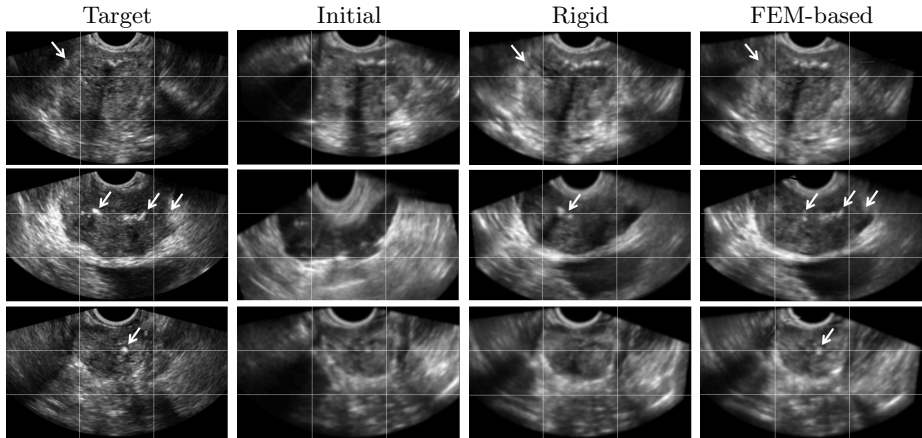

| Target | Initial | Rigid | FEM-based |

Fig. 3. Typical registration results for three patients (top, middle and bottom rows). The first column denotes the live 2D-TRUS (target) images. The next three columns show the initial alignment using the trajectory, rigid registration, and FEM-based registration results, respectively. White arrows indicate locations where the registration framework shows improvements.

3   Experiments and Results

The proposed 2D-3D registration was evaluated on 10 patients. The systematic sextant biopsy protocol in our hospital requires the acquisition of 8–12 distributed cores, with extra cores in suspicious regions. For the patients in this study, this yielded a total of 10 pre-procedure TRUS volumes and 115 2D TRUS slices at biopsy cores. To quantify registration error, we computed the Euclidean distance between intrinsic fiducials, consisting of micro-calcifications and cysts (Figure 2). A total of 65 fiducials were identified.

Figure 3 shows registration results for three patients. In the top-row, rigid registration performs well, however, there is a slight improvement near the prostate boundary following FEM-based registration. The middle-row shows an example where FEM-based registration corrects for the boundary and brings additional structures into the registration plane. In the bottom-row, FEM-based registration is required to correctly identify the calcification.

Table 1. Registration results and p-value to investigate statistical significance.

TRE, mean $\pm$ s.d. (mm)			$p-$value	
Initial	Rigid	FEM-based	Initial vs. Rigid	Rigid vs. FEM-based
6.31 ± 1.86	4.63 ± 1.05	3.15 ± 0.82	$p < 10^{-4}$	$p < 10^{-5}$

As seen in Table 1, rigid and FEM-based registration reduce the mean TRE from the initial 6.31 mm down to 4.63 mm and 3.15 mm, respectively. This suggests that substantial biomechanical deformations exist and can be compensated for using our FEM-based approach. To investigate the statistical significance of TRE reduction, we first checked if the TREs were normally distributed. Using the one-sample Kolmogorov-Smirnov test, we found that the distribution of the TRE is not normal at the 5% significance level for initial, rigid and FEM-based methods ($p < 10^{-4}$). Therefore, we performed a signed Wilcoxon rank sum test. The $p-$value from this experiment is also shown in Table 1. The test rejected the hypothesis that TREs for initial vs. rigid and rigid vs. FEM-based methods belong to a distribution with equal medians. Therefore, the improvements in mean TRE following rigid and FEM-based registration are statistically significant.

4   Discussion and Conclusions

We presented a novel registration framework for motion and deformation compensation during a freehand TRUS-guided prostate biopsy. The improvement in the TRE using the FEM-based registration should be compared to the acceptable error bounds of a 3D prostate biopsy system. A TRE of 2.5 mm yields a confidence interval in which 95% of registered targets come within the smallest clinically significant tumor [4]. The result of our FEM-based registration (3.15 mm) brings us closer to this acceptable error bound. In our study, no instructions were given to the radiologist to control the probe pressure. If the biopsy protocol is slightly modified to maintain a low probe pressure, it should be possible to decrease the error closer to a clinically acceptable range [4].

Our next steps aim to increase the accuracy of the proposed framework. Since the quality of the pre-procedure volume directly affects registration results [7], we wish to tackle challenges associated with deformation artifacts due to breathing and inconsistent probe pressure, including estimating a "rest shape" of the prostate using shape statistics, and validating the reconstructed volume against magnetic resonance images. Another direction is to perform multi-slice registration, which has been shown to improve the TRE [2,7], and compare our non-rigid registration approach to other methods [7]. The current run-times of the rigid and FEM-based components of our framework are in the order of ≈ 30 seconds and ≈ 10 minutes, respectively. Decreasing the registration time can be accomplished by calculating the terms in Equation (3) in parallel per pixel on a graphics processing unit, by adopting a multi-resolution approach, and by performing registration continuously during the procedure [4]. This would allow us to integrate the registration framework into the biopsy procedure, so it can be validated on a larger cohort of patients.

References

1. Baumann, M., Mozer, P., Daanen, V., Troccaz, J.: Prostate biopsy tracking with deformation estimation. Medical Image Analysis 16(3), 562–576 (2012)
2. De Silva, T., Cool, D.W., Romagnoli, C., Fenster, A., Ward, A.D.: Evaluating the utility of intraprocedural 3D TRUS image information in guiding registration for displacement compensation during prostate biopsy. Medical Physics 41(8), 082901 (2014)
3. De Silva, T., Cool, D.W., Yuan, J., Romognoli, C., Fenster, A., Ward, A.D.: Improving 2D-3D registration optimization using learned prostate motion data. In: Mori, K., Sakuma, I., Sato, Y., Barillot, C., Navab, N. (eds.) MICCAI 2013, Part II. LNCS, vol. 8150, pp. 124–131. Springer, Heidelberg (2013)
4. De Silva, T., Fenster, A., Cool, D.W., Gardi, L., Romagnoli, C., Samarabandu, J., Ward, A.D.: 2D-3D rigid registration to compensate for prostate motion during 3D TRUS-guided biopsy. Medical Physics 40(2), 022904 (2013)
5. Hu, Y., Ahmed, H.U., Taylor, Z., Allen, C., Emberton, M., Hawkes, D., Barratt, D.: MR to ultrasound registration for image-guided prostate interventions. Medical Image Analysis 16(3), 687–703 (2012)
6. Kemper, J., Sinkus, R., Lorenzen, J., Nolte-Ernsting, C., Stork, A., Adam, G.: MR elastography of the prostate: initial in-vivo application. Fortschr Röntgenstr 176(08), 1094–1099 (2004)
7. Khallaghi, S., Nouranian, S., Sojoudi, S., Ashab, H.A., Machan, L., Chang, S., Black, P., Gleave, M., Goldenberg, L., Abolmaesumi, P.: Motion and deformation compensation for freehand prostate biopsies. In: Proc. SPIE, vol. 9036, pp. 903620–903626 (2014)
8. Lasso, A., Heffter, T., Rankin, A., Pinter, C., Ungi, T., Fichtinger, G.: Plus: Open-source toolkit for ultrasound-guided intervention systems. IEEE Transactions on Biomedical Engineering 61(10), 2527–2537 (2014)
9. Leite, K.R.M., Camara-Lopes, L.H., Dall'Oglio, M.F., Cury, J., Antunes, A.A., Sañudo, A., Srougi, M.: Upgrading the gleason score in extended prostate biopsy: implications for treatment choice. International Journal of Radiation Oncology Biology Physics 73(2), 353–356 (2009)
10. Marami, B., Sirouspour, S., Ghoul, S., Cepek, J., Davidson, S.R., Capson, D.W., Trachtenberg, J., Fenster, A.: Elastic registration of prostate MR images based on estimation of deformation states. Medical Image Analysis 21(1), 87–103 (2015)
11. Wang, Y., Ni, D., Qin, J., Lin, M., Xie, X., Xu, M., Heng, P.A.: Towards personalized biomechanical model and MIND-weighted point matching for robust deformable MR-TRUS registration. In: Luo, X., Reich, T., Mirota, D., Soper, T. (eds.) CARE 2014. LNCS, vol. 8899, pp. 121–130. Springer, Heidelberg (2014)
12. Xu, S., Kruecker, J., Turkbey, B., Glossop, N., Singh, A.K., Choyke, P., Pinto, P., Wood, B.J.: Real-time MRI-TRUS fusion for guidance of targeted prostate biopsies. International Society for Computer Aided Surgery 13(5), 255–264 (2008)
13. Yan, P., Xu, S., Turkbey, B., Kruecker, J.: Adaptively learning local shape statistics for prostate segmentation in ultrasound. IEEE Transactions on Biomedical Engineering 58(3), 633–641 (2011)